

## GT2011-46614

### Discussion about the Practice of Using a Heated Surface in Film Cooling Studies

Lei Zhao and Ting Wang

Energy Conversion and Conservation Center  
 University of New Orleans  
 New Orleans, LA 70148-2220, USA  
 E-mails: [lzhao@uno.edu](mailto:lzhao@uno.edu); [twang@uno.edu](mailto:twang@uno.edu)

#### ABSTRACT

It is found in many film-cooling experiments and computational analyses that a heated surface is employed to simulate the actual film-cooling condition with a cooling jet and a hot main flow. Considering that the dominant energy passage in turbine airfoil film cooling is always from the hot combustion gas flowing into the airfoil, employing a heated surface to simulate the actual film cooling condition does not provide the correct physics of the heat flow under an actual film cooling condition, and therefore, the results are questionable. The objective of this paper is to investigate the consequent results associated with the practice of employing a heated surface by comparing its result with actual conditions including a conjugate metal wall and internal cooling via a series of computational simulations.

When the surface is heated, in some conditions, negative film cooling effectiveness can be found as a result of a higher surface temperature than the main gas stream temperature. This is unrealistic for an operational turbine system. The heated wall acts as an active heat source; as a result, the concept of using the adiabatic wall temperature ( $T_{aw}$ ) as the driving temperature potential is no longer valid because an artificially created competing heat source is added into the system, and the heat transfer mechanism on the airfoil is not solely determined by  $T_{aw}$ .

Heating the surface to simulate the film cooling boundary condition, although it does not provide correct physics, can provide the heat transfer coefficient value within 10-15% of the value calculated from the correct boundary conditions. Using a heated surface is only correct under one condition: when all the conditions are reversed, i.e. with a hot jet and cold main gas flow.

The practice of using a jet flow with the same temperature of the hot gas (isoenergetic jet) to obtain the film heat transfer coefficient will result in about 20-25% discrepancy from the cooling jet case. The uniformly cooled wall cases fair better than heated cases because it provides correct physics in most part of the surface.

#### NOMENCLATURE

b coolant injection slot width (mm)

$h_{af}$  adiabatic film heat transfer coefficient ( $h_{af} = q'' / (T_{aw} - T_w)$ ) ( $W/m^2K$ )  
 HFR heat flux ratio ( $q'' / q''_o$ )  
 l chord length (mm)  
 M blowing ratio,  $(\rho u)_j / (\rho u)_g$   
 $Nu_x$  Nusselt number,  $hx/\lambda$   
 NHFR net heat flux reduction ( $1 - q'' / q''_o$ )  
 $Pr$  Prandtl number ( $\nu/\alpha$ )  
 $q''$  heat flux ( $W/m^2$ ), positive value for heat flowing from gas into the wall  
 r recovery factor  
 $Re_l$  Reynolds number based on chord length,  $ul/\nu$   
 $T_{aw}$  adiabatic wall temperature (K)  
 $T_w$  wall surface temperature in contact with gas (K)  
 $T_g$  main gas flow temperature (K)  
 $T_j$  coolant temperature at the cooling jet hole exit (K)  
 $T_{ci}$  internal coolant temperature (K)  
 $T_r$  recovery temperature (K)  
 $T_u$  turbulence intensity

#### Greek Letters

$\eta$  adiabatic film cooling effectiveness,  $(T_g - T_{aw}) / (T_g - T_j)$   
 $\lambda$  heat conductivity ( $W/mK$ )  
 $\phi$  film cooling effectiveness,  $\phi = (T_g - T_w) / (T_g - T_j)$  (or non-dimensional metal temperature)

#### Subscript

aw adiabatic wall  
 ci internal cooling  
 conj conjugate blade  
 f with film cooling  
 g main flow of hot gas/air  
 j coolant or jet flow  
 o without film  
 w wall

#### INTRODUCTION

Film cooling has been widely used in high-performance gas turbines to protect turbine airfoils from being damaged by hot flue gases. Film injection holes are placed in the body of the airfoil to allow coolant to pass from the internal cavity to the external surface. The ejection of coolant gas results in a layer or

“film” of coolant gas flowing along the external surface of the airfoil. Hence, the term “film cooling” is used to describe this cooling technique.

The ultimate goal of introducing film cooling to turbine airfoils is to reduce the heat load on the blade, i.e. to reduce the surface heat flux and/or lower the airfoil's temperature, so that the life of the turbine airfoils can be significantly extended due to lower thermal stress within the material and less spallation over the thermal barrier coating due to a lower thermal load. Thus it is always desired to know how much heat flux or blade temperature can be actually reduced after film cooling is employed. However, due to the experimental difficulty in directly measuring the heat flux, the **Heat Flux Ratio (HFR)**  $q'' / q''_o$  is often evaluated indirectly through a theoretical relation developed by Mick and Mayle [1] between two characteristic factors of film cooling heat transfer: adiabatic film effectiveness ( $\eta$ ) and film heat transfer coefficients ( $h_{af}$  and  $h_o$ ), as:

$$q'' / q''_o = (h_{af} / h_o) (1 - \eta / \phi) \quad (1)$$

In which, the **adiabatic film effectiveness** is defined as:

$$\eta = (T_g - T_{aw}) / (T_g - T_j) \quad (2)$$

Where  $T_g$  is the main flow hot gas temperature,  $T_j$  is the coolant temperature at the cooling jet hole exit, and  $T_{aw}$  is the adiabatic wall temperature.  $\eta$  is an excellent indicator of film cooling performance by comparing the insulated wall surface temperature ( $T_{aw}$ ) with the would-be perfect wall temperature,  $T_j$ . If the film cooling were perfect,  $\eta = 1$  and the wall is protected to maintain as cold as the cooling jet. The **adiabatic film heat transfer coefficient** is defined as:

$$h_{af} = q'' / (T_{aw} - T_w) \quad (3)$$

In Eq. 1,  $q''_o$  is the local heat flux without film cooling, and  $h_o$  is given as:

$$h_o = q''_o / (T_g - T_w) \quad (4)$$

the **film cooling effectiveness**,  $\phi$ , is defined as:

$$\phi = (T_g - T_w) / (T_g - T_j) \quad (5)$$

To reduce complexity,  $T_j$  is assumed the same as the internal coolant temperature,  $T_{cj}$ . Although we can say that  $\eta$  is a special case of the more generically defined film cooling effectiveness ( $\phi$ ) when the wall is insulated, it is convenient to use both terms by designating  $\phi$  for all non-adiabatic wall conditions and  $\eta$  only for the adiabatic wall condition.  $\phi$  has also been called the **non-dimensional metal temperature** (The Gas Turbine Handbook [2]) or the **overall cooling effectiveness** in other literatures.

For a perfect film cooling performance, the film cooling effectiveness would have a value of unity ( $\eta$  or  $\phi = 1.0$ ), i.e.  $T_{aw}$  is equal to the coolant temperature ( $T_j$ ) at the exit of the jet injection hole; while a value of  $\eta = 0$  means that the film cooling has no effect in reducing the wall temperature, which is heated to the same temperature as the mainstream gas.

In a real gas turbine condition, the airfoils are cooled inside by an internal coolant flow and almost all the coolant is bled and utilized for film cooling. Therefore, the actual heat transfer path

goes through a conjugate condition from the hot main flow gas to the airfoil surface via convection and radiation, spreads over the airfoil via conduction, and then transfers to the internal cooling fluid via convection again. The ultimate energy source is the main flow of hot gases and the energy sinks are the internal flow and film flow. Due to the complexity of this conjugate heat transfer condition, many film cooling experiments have been performed under simplified conditions such as applying an isothermal condition or uniformly heated wall condition.

Isothermal (isoenergetic) film cooling is named for the condition where  $T_j = T_g$ , i.e., the jet is as hot as the gas stream. Conventionally, the  $h_{af}$  value is obtained by conducting an isothermal film experiment. There are numerous examples such as the studies of Burd et al. [3] and Thurman et al. [4]. Since  $h_{af}$  should include the effects from the film-disturbed flow field and thermal field, an isothermal film experiment only provides the effect of the flow field, which actually helps enhance the heating of the surface instead of the cooling because the film jet promotes turbulence and augments surface heating. While the jet flow-induced mixing, which changes the film distribution and concentration, acts adversely to the goal of reducing heat flux through film cooling, the lower coolant temperature serves to protect the surface by absorbing the heat from the main flow. These two mechanisms compete with each other, and it is therefore essential to distinguish the difference between the effects of flow field from the effect of lower temperature on film cooling performance. Consequently, the overall performance of film cooling manifests a net wall heat flux reduction which takes into account decreased gas temperature provided by the coolant film and the increased heat transfer coefficient due to the hydrodynamic effect of coolant injection process.

In the isothermal film case, the actual heat transfer coefficient should be evaluated as  $h = q'' / (T_g - T_w)$ ; however, in order to fit the definition in Eq 1,  $h_{af}$  is calculated via Eq. 3 instead of  $h$ . In this practice, two issues are raised. First, the  $h_{af}$  so obtained does not include the effect of the actual jet coolant temperature,  $T_j$ , so  **$h_{af}$  is overvalued** because  $T_w$  should be lower if  $T_j$ 's temperature effect is included. Second, in the isothermal film experiment, the wall heat flux needs to be measured. If  $q''$  can be measured, why not just use a lower-temperature coolant to perform the experiment and obtain the actual film-cooled heat flux without even bothering to use Eqs. 1 and 2 or run the adiabatic case? The reason is that an accurate measurement of heat flux is not easy under a conjugate condition, so most of the studies employ a uniformly heated surface to simulate the isothermal film heat transfer study. Implicitly, the experiment reverses the heat path by transferring heat from the wall to the free-stream. This practice is acceptable with the above condition when  $T_j = T_g$ , but it leads to the next issue when  $T_g > T_j$ .

Conventionally, many film-cooling experiments and computational analyses have used a heated surface to simulate the actual film-cooling condition with a cooling jet and a hot main flow. One of the motivations of using this approach is to take advantage of the convenience of controlling the constant heat release without actually measuring the local heat flux or employing conjugate cooling below the surface. This practice is also based on the observation that the airfoil surface is usually hotter than the film temperature, so it seems appropriate and convenient to simplify the conjugate condition with a heated surface. Some examples of the group of experiments are the studies of Jonsson et al. [5] and Nicklas et al. [6]. This simplified practice is seemingly fine, but a close examination of the physics

leads to an unwelcome negative conclusion: a heated surface with a cooling jet and hot gas does not provide the correct physics of the heat flow under an actual film cooling condition and therefore the results are questionable. This means that in the real film-cooled surface, the heat is transferred from the gas to the wall, which is the opposite of the heated flow experimental case where the heat transfers from the wall to the gas. It is easy to fall into the trap of thinking that the cooling film has a temperature lower than the wall, so the heat tends to transfer from the “hot” wall surface to the cooling air. The reality is that the cooling air, which mixes with the hot main stream gas, reduces the bulk temperature near the wall and hence reduces the heat transferred to the wall, but the mixture temperature is still higher than the wall temperature with an exception of the limited area where the wall temperature is higher than the near-wall gas due to heat conduction in the wall. The small region of reversed heat transfer has been reported by Mouzon et al. [7] and Coulthard et al. [8] and will be discussed and simulated by CFD later.

As has been emphasized, the only energy source in the actual film cooling condition is the main flow hot gas, so if there is a path for heat to transfer from the surface back to the gas flow, it must be the result of the natural course of the heat transfer. This means that the reason that the surface becomes hot must be due to accessible heat paths from the main gas flow to the surface. These heat paths can be contributed to by turbulent eddies penetrating through to the surface, secondary flows wrapping from the lateral direction, radiation, or pure diffusion of heat to the surface. Typically the gas temperature adjacent to the wall would be higher than the wall surface temperature and the chance for heat transferring back from the surface to the gas must only be provided by the conduction inside the wall material that redistributes the heat from the hotter region to the colder region. This heat conduction path makes the wall surface temperature warmer than the adjacent gas temperature immediately away from the wall. Therefore, using a heated wall as the wall boundary condition is only valid for the limited area (usually near the film hole) where the wall temperature is hotter than the near-wall gas temperature.

The heated wall can be used as the correct boundary condition only if all the heat flow directions are consistently reversed, i.e. using a heating jet with a temperature higher than the main gas stream ( $T_j > T_g$ ). Mick and Mayle [1] did just this by adopting a completely reversed heat flow condition in their study. The completely reversed system can also be found in some recent studies, for example in Burd at al. [3] and Womack et al. [9].

If the heated surface condition is employed for the purpose of obtaining  $h_{af}$  only, another concern is raised to the effect of variable properties since the temperature gradient is totally opposite from the real condition with the airfoil surface being cooled: the flow field, fluid properties, and heat transfer might be altered, especially in the near wall region. This concern can be investigated by examining  $h_{af}$ , obtained through both heated and cooled surface cases in this study.

A sketch is shown in Fig. 1 to qualitatively illustrate the heat transfer scenario including the temperature profiles at two locations: one near the jet injection hole with a possible reversed heat flow and the other located further downstream from the injection hole region. The slopes of the temperature profiles are drawn to qualitatively reflect the heat flow direction.

The objective of this paper is to systematically investigate the above issues guided by CFD simulations.

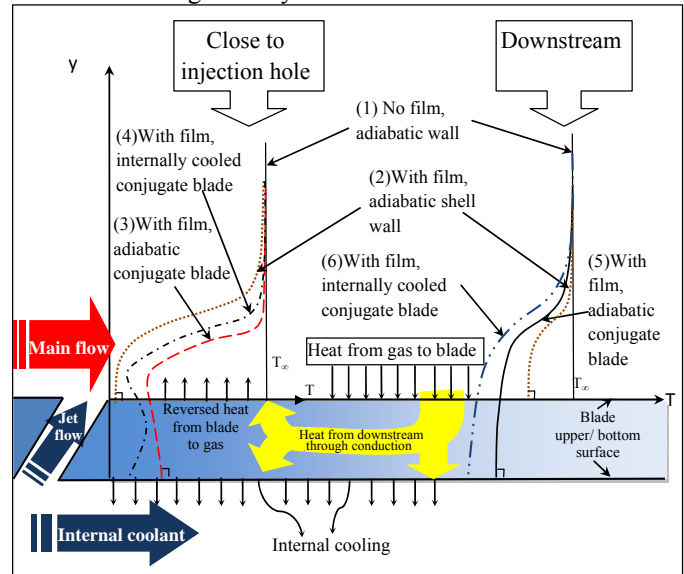


**Figure 1 A qualitative illustration of temperature profiles of a typical internally and film cooled blade at two locations: one near the injection hole region with potentially reversed heat transfer and the other located further downstream. The axial heat conduction transfer is small and the size of reversed heat flux arrowhead is enlarged for illustration purpose.**

## MODELING AND METHODOLOGY

The investigation in this paper is guided by a series of computational fluid dynamic (CFD) simulations. Although the actual numerical values of CFD are often subject to uncertainty due to different turbulence models, discretization resolution, and grid quality, the global heat transfer and flow physics can be captured relatively trustfully in modern CFD schemes. Since the focus of this study is on the thermal-flow physics and relative comparisons of different cases, any bias generated by the CFD scheme is generally not so critical in the comparative nature of the analysis conducted in this paper.

Considering that experimental film cooling studies using low temperature and low heat flux laboratory conditions have been more commonly seen in open literatures than those employing real engine conditions, in this study the issues will be discussed based on simulations of lab conditions. While quite obviously in real engine conditions, which are characterized by elevated pressure, temperature, heat flux, and flow speed conditions, the properties of the airfoil wall material and fluid flow will differ from those in the lab conditions. But since the discussions are based on normalized values of  $\phi$  and  $\eta$  and are focused on the methodology of practices, using data in lab conditions should not change the physics and issues extensively discussed in this paper. The elevated conditions will only affect the quantitative values of  $\eta$  and  $\phi$ , but not the fundamental physics and methodology investigated in this paper. For example, as shown in the study of Wang and Zhao [10], in certain real engine conditions, the  $\phi$ -value could change from 0.6 to another value and the area of reversed heat transfer may expand a bit, but the issues and conclusions would not be affected.

## Geometrical Configuration

To make the analysis easier, 2D conditions with various changing parameters are simulated first; 3D cases will follow to add the impacts from the complexity of the 3D flow structure. In the 2D cases, a slot is selected; its configuration and the main dimensions are shown in Fig. 2. A 3D study is then built upon the geometry set-up of the 2D studies, with a pitch to diameter ratio ( $p/b$ ) of 3. It needs to be noted that cylindrical hole is used in 3D which is different from the slot injection in 2D.

The slot width ( $b$ ) is 4 mm. The injection angle is  $35^\circ$ , which is considered to be the optimal value by Bell et al. [11] and Brittingham et al. [12]. The length of the film slot is  $3b$  from the coolant supply plenum to the surface. The computational domain has a length of  $80b$  and a height of  $20b$ . The slot jet is set to  $20b$  from the entrance of the mainstream. In the arrangement of the conjugate cases, the solid metal wall with a uniform thickness of  $1.72b$  is included in the computational domain. An internal cooling channel flow is imposed below the base wall bottom surface, with an internal heat transfer coefficient  $h_i$  and a coolant flow temperature  $T_{ci}$  as shown in Fig. 2. It is understood that the plenum and film injection hole conditions have important effects on film cooling performance and there are numerous research papers focusing on those topics, but since this paper is not aimed for studying film cooling performance, and also for the purpose of simplifying the analysis and focusing on the HFR issues, a plenum is not included and the adiabatic wall condition is assumed within the film injection wall.

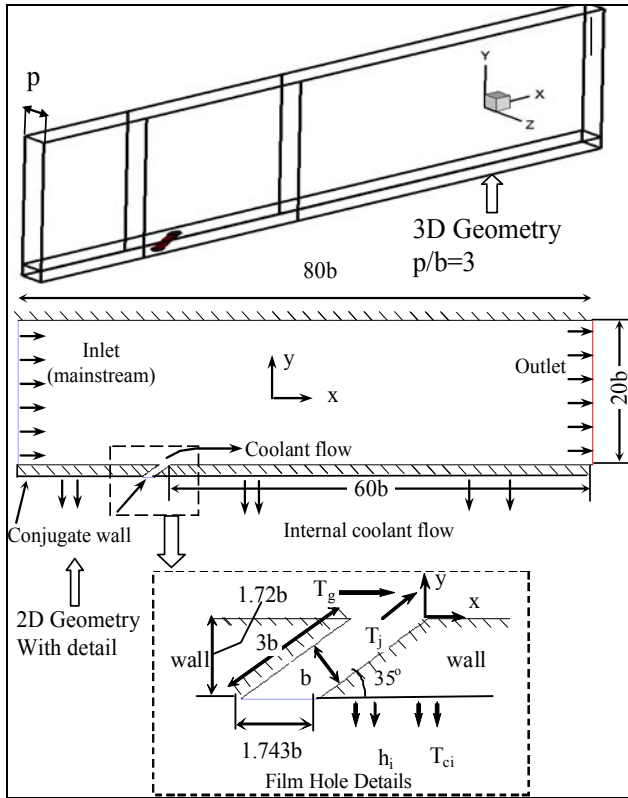


Figure 2 Computational domains for 2D and 3D respectively

## Governing Equations

The time-averaged, steady state Navier-Stokes equations as well as equations for mass and energy are solved. The

governing equations for conservation of mass, momentum, and energy are given as:

$$\frac{\partial}{\partial x_i}(\rho u_i) = S_m \quad (6)$$

$$\frac{\partial}{\partial x_i}(\rho u_i u_j) = \rho \bar{g}_j - \frac{\partial P}{\partial x_j} + \frac{\partial}{\partial x_i}(\tau_{ij} - \rho \overline{u'_i u'_j}) + F_j \quad (7)$$

$$\frac{\partial}{\partial x_i}(\rho c_p u_i T) = \frac{\partial}{\partial x_i} \left( \lambda \frac{\partial T}{\partial x_i} - \rho c_p \overline{u'_i T'} \right) + \mu \Phi + S_h \quad (8)$$

where  $\tau_{ij}$  is the symmetric stress tensor defined as:

$$\tau_{ij} = \mu \left( \frac{\partial u_j}{\partial x_i} + \frac{\partial u_i}{\partial x_j} - \frac{2}{3} \delta_{ij} \frac{\partial u_k}{\partial x_k} \right) \quad (9)$$

$\mu \Phi$  is the viscous dissipation and  $\lambda$  is the thermal conductivity.

Notice the terms of  $\rho \overline{u'_i u'_j}$ , and  $c_p \overline{u'_i T'}$  represent the Reynolds stresses and turbulent heat fluxes, which should be modeled properly for a turbulent flow.

## Boundary Conditions

All walls have a non-slip velocity boundary condition in this study. Flow conditions with low temperature, pressure, and velocity for typical laboratory experiments are employed. For conjugate cases, Inconel X-750 properties are used for the blade material with variable properties as functions of temperature. A heat transfer coefficient of  $h_i = 100 \text{ W/m}^2\text{-K}$  and coolant flow temperature  $T_{ci} = 300\text{K}$  are assigned to the internal cooling flow, which is located at the bottom of Fig. 2. Air is modeled as an incompressible ideal gas with the density varying with temperature and the heat capacity modeled as a piecewise polynomial function of temperature with two temperature sub-ranges of 100-1000K and 1000-2000K, respectively. Inlet and outlet conditions and wall thermal boundary conditions for the cases under lab conditions are summarized in Table 1. Details of the cases' set-up will be shown later in this section.

Table 1 Summary of Boundary Conditions

		2-D hole	
Operational pressure	$P$ (atm)	1	
Main stream inlet	$T_g$ (K)	400	400K=260.6°F
	$u_g$ (m/s)	10	Uniform
	$Tu$ (%)	3	Turbulence Intensity
	$Re_1 \times 10^{-6}$	0.21	$l=0.32\text{m}$
Jet inlet	$T_j$ (K)	300	300 K = 80.6°F
	$u_j$ (m/s)	10	Uniform
	$Tu$ (%)	3	Turbulence intensity
	$Re_d \times 10^{-3}$	2.67	$d=4\text{mm}$
$M=(\rho u)_j/(\rho u)_g$	$M$	1.3	blowing ratio
Outlet	$P$ (atm)	1	Constant pressure
Conjugate cooling wall	$T_{ci}$ (K)	300	
	$h_i$ (W/m <sup>2</sup> -K)	100	
Constant temperature wall	$T_w$ (K)	325	$\phi=0.75$
	$T_w$ (K)	375	$\phi=0.25$
Uniformly cooled wall	$q''$ (W/m <sup>2</sup> )	3000	Constant heat flux
	$q''$ (W/m <sup>2</sup> )	6000	
Uniformly heated wall	$q''$ (W/m <sup>2</sup> )	-3000	Constant heat flux
	$q''$ (W/m <sup>2</sup> )		

## Numerical Method

The commercial software code Fluent (version 6.2.16) from Ansys, Inc. is adopted in this study. The simulation uses the segregated solver, which employs an implicit pressure-correction scheme [13]. The SIMPLE algorithm is used to couple the

pressure and velocity. The second order upwind scheme is selected for spatial discretization of the convective terms.

As shown in Fig. 3, structured but non-uniform meshes are constructed for 2-D studies. The meshes near the jet wall and the wall surface are denser than the other areas. A grid independence study is conducted by comparing the adiabatic film effectiveness of simulations based on two different mesh sizes of 80,000 and 48,000 cells. The results are almost identical. The mesh adopted in this study is of 400 cells in the x-direction and 120 in the y-direction for 2D studies. Unstructured grids are employed for the 3-D studies with finer meshes near the injection hole and the top surface. Less than 5% difference in the adiabatic film effectiveness on the centerline is found from the simulations based on meshes of 1.24 million cells versus 772,000 cells.

Converged results are obtained after the specified residuals are met. A converged result renders a mass residual of  $10^{-5}$ , an energy residual of  $10^{-7}$ , and momentum and turbulence kinetic energy residuals of  $10^{-6}$ . These residuals are the summation of the imbalance for each cell, scaled by a representative of the flow rate. Typically, 1000 to 2000 iterations are needed to obtain a converged result, which takes about 2 hours on a parallel computer cluster consisting of eight nodes of 2.53 GHz Pentium dual-core personal computers.

#### CFD Model Qualification and Uncertainty Estimate

The CFD benchmark case using the current 3D grid is carried out. The simulation results are compared with the experimental data of Goldstein et al. [14]. The spanwise-averaged adiabatic film cooling effectiveness for the case  $M = 0.5$  is used for comparison. Also, the effect of turbulence models using the same 3D grid is investigated. Five turbulence models are studied and the results are plotted in Fig 3b. The standard k- $\epsilon$  model with enhanced near-wall treatment gives the best agreement with the experimental data and is hereby employed in this study. The  $Y^+$  values of the first near-wall cell from the qualification case are below 0.8 for most X locations.

The uncertainty from the key factors are estimated as: 10% for the 3 different turbulence models, 5% for the turbulence length scales, 3% for resolution of the second order central and upwind methods, 1% for convergence resolution, 5% for the effect of grid size, and 3% for the near-wall grid effect. The overall uncertainty for cooling effectiveness is estimated to be 13% using the root-mean-square method. The above uncertainty is estimated from the computational results under low temperature and pressure conditions. Therefore, the estimated uncertainty is not centered with the true value; rather it represents the uncertainty excursion of the results that are attributed by the computational model and scheme.

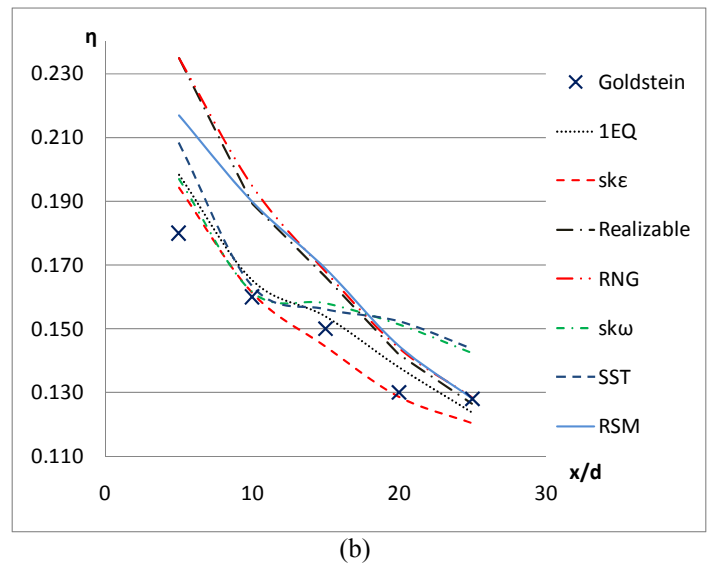
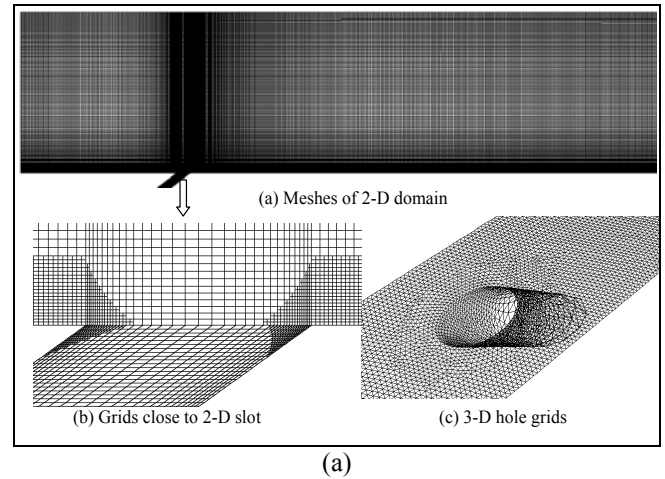


**Figure 3 (a) Computational Meshes for 2D and 3D, respectively (b) Comparison of CFD result with the experimental result of Goldstein [14]**

#### Methodology and Cases Set-up

The conjugate heat transfer scenario of an operational turbine airfoil film cooling system consists of a main flow of hot gas with known conditions riding along the airfoil's upper surface, an internal coolant flow moving underneath the airfoil's bottom surface, and a portion of the coolant being injected through the coolant holes over the airfoil surface. The airfoil wall temperature and heat flux are determined by those conditions. The most appropriate simulation of this film-cooling system is to set up the main flow, internal flow and film injection conditions as boundary conditions while leaving the airfoil's wall thickness as part of the conjugate calculation.

The heat flux is calculated from the simulation based on the temperature results,  $q'' = -k(dT/dy)$  at wall.  $(dT/dy)$  is calculated by the wall surface temperature and the adjacent cell temperature, which are both computed by CFD. The  $k$  value is calculated based on local temperature.

Also to evaluate the heat transfer coefficient change due to the addition of film, the heat transfer of the same system running without film injection needs to be simulated. The conjugate cases described above are set as the baseline cases. The adiabatic

wall case is also simulated so that  $T_{aw}$  is obtained to evaluate  $h_{af}$  from Eq. 3.

As discussed in the previous section, for the convenience of setting up an experiment, a simplified experimental test section has been often employed by imposing a heated or cooled boundary condition. Concerns on this simplified practice have been discussed in the introduction section, and to investigate the issues involved, three cases with uniformly heated and cooled conditions with  $q'' = \pm 3$  and  $+6$  kW/m<sup>2</sup> are simulated. Also since constant temperature walls are often adopted in experiments, two cases of constant wall temperature  $T_w = 325$ K and  $375$ K (corresponding to  $\phi = 0.75$  and  $0.25$ , respectively) are also studied in this paper. These five cases are simulated both with and without film conditions. An isothermal condition is also simulated with  $T_j = T_g$ . The 2D cases are summarized in Table 2 with an illustration drawn in Fig. 4. A conjugate case with internal cooling, an adiabatic wall case, uniformly heated and cooled cases with  $q'' = \pm 3$  and  $6$  kW/m<sup>2</sup>, and an isothermal case are also investigated in 3D simulations. The set-up of the 3D cases is similar to that of the 2D cases, so they are not listed in Table 2.

**Table 2 Summary of Cases Set-up**

Case #	Film Existence	Thermal Boundary Condition
Case 1.1	without film	internal cooling, conjugate
Case 1.2	with film	internal cooling, conjugate
Case 2	with film	adiabatic
Case 3.1	without film	constant T wall, $T_w = 325$ K
Case 3.2	with film	constant T wall, $T_w = 325$ K
Case 4.1	without film	constant T wall, $T_w = 375$ K
Case 4.2	with film	constant T wall, $T_w = 375$ K
Case 5.1	without film	uniformly cooled wall, $q'' = +3$ kW/m <sup>2</sup>
Case 5.2	with film	uniformly cooled wall, $q'' = +3$ kW/m <sup>2</sup>
Case 6.1	without film	uniformly cooled wall, $q'' = +6$ kW/m <sup>2</sup>
Case 6.2	with film	uniformly cooled wall, $q'' = +6$ kW/m <sup>2</sup>
Case 7.1	without film	uniformly heated wall, $q'' = -3$ kW/m <sup>2</sup>
Case 7.2	with film	uniformly heated wall, $q'' = -3$ kW/m <sup>2</sup>
Case 8	with film	Isoenergetic, $T_g = T_j$

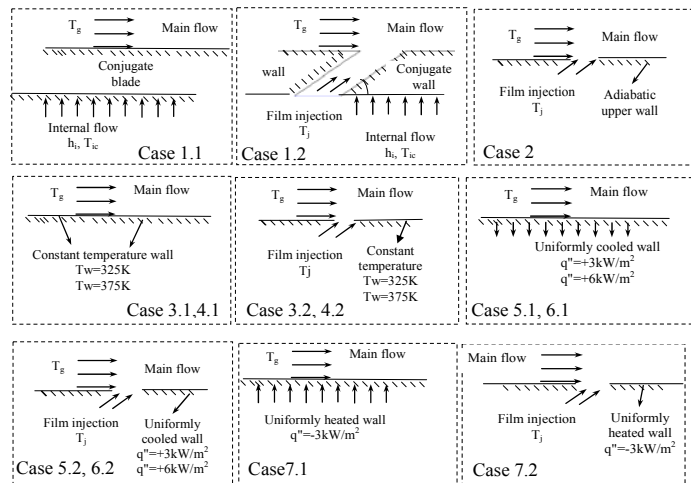


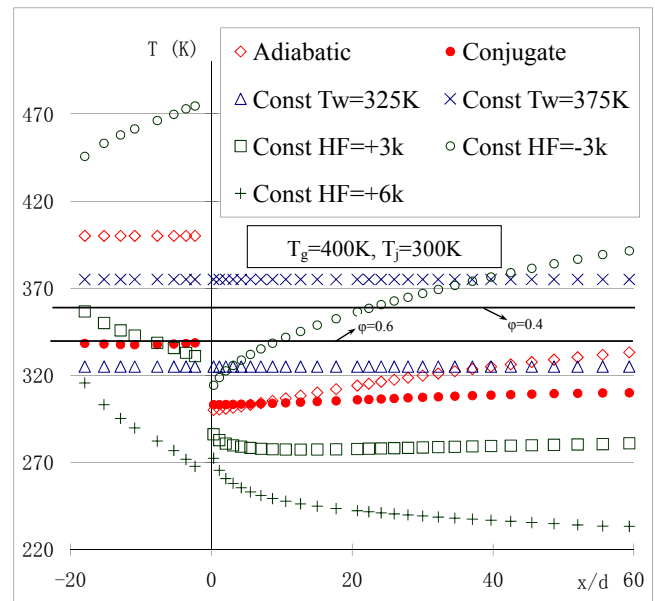
**Figure 4 Illustrations of boundary condition set-up for different cases**

## RESULTS AND DISCUSSIONS

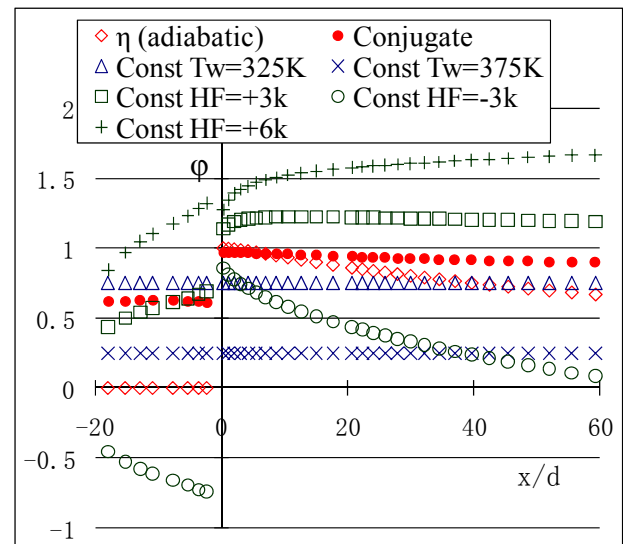
### Discussion on Using Heated or Cooled Wall Conditions for Film Cooling Experimental Setup

The results of wall temperature and film cooling effectiveness for 2D cases with different boundary conditions are shown in Fig. 5 and discussed below.

**Conjugate Case** --- It is noticed that  $\phi_{conj}$  is slightly lower than  $\eta$  in a small area immediately downstream of the jet hole and is higher than  $\eta$  in the rest of the downstream region. A higher value of  $\phi$  indicates a better film cooling effect. Thus, a higher  $\phi_{conj}$  compared with  $\eta$  means a better cooling effect is achieved in the conjugate case than the adiabatic wall case. The extra cooling effect comes from the internal cooling included in the conjugate case. However  $\phi_{conj}$  is lower than  $\eta$  in the neighborhood of the jet hole area because the conduction effect through the wall transfers heat from the hotter downstream region to the cooler upstream area and overpowers the internal cooling effect. Upstream of the film hole,  $\phi_{conj}$  value is about  $0.6$ , indicating the effect of internal cooling without the film cooling effect.



(a)



(b)

**Figure 5 2D (a) adiabatic wall temperature and wall temperature (b) film cooling effectiveness ( $\phi$ ) and adiabatic film cooling effectiveness ( $\eta$ ) under different wall conditions.**

Uniformly Cooled Wall Cases --- For the two uniformly cooled wall cases with heat fluxes at  $3\text{kW/m}^2$  and  $6\text{kW/m}^2$ , it is noticed that in the area downstream of the film hole,  $\phi$  values are greater than 1, which is not realistic in a typical cooled turbine airfoil system. As discussed in the introduction section,  $\phi$  equals unity means the airfoil surface is as cool as the film jet temperature and  $\phi$  greater than one indicates that the heat sink imposed on the wall exceeds the maximum cooling power of the actual system and results in an unreal lower wall temperature than the coolant temperature.

Looking at upstream temperature of the cooled wall case at  $3\text{kW/m}^2$ ,  $\phi$  is less than 1, which correctly indicates the convective cooling effect by the wall. A jump of increased value of  $\phi$  crossing the coolant hole is seen, indicating that additional cooling effect is provided by the film injection than the imposed cooled wall condition near the coolant hole area. Meanwhile the jump is less noticeable in the stronger cooling case ( $6\text{kW/m}^2$ ), meaning that film injection does not contribute much to an already more strongly cooled wall.

Uniformly Heated Wall Cases --- A negative  $\phi$  value is found upstream of the film hole. This is resulted from a higher wall temperature than the main stream temperature, which is a natural feature of an actively heated wall condition because the wall is the heat source, but the negative  $\phi$  value is unrealistic for an operational turbine system.

$\phi$  jumps from the unrealistic negative values to reasonable values crossing the film injection hole, indicating the significant effect of film cooling.  $\phi$  is lower than the adiabatic case, showing a less effective film cooling performance over a heated wall comparing with an insulated wall. The heated wall arrangement also preheats the coolant film, resulting in a significantly reduced overall cooling effect. From this analysis, it is clear that the practice of heating the wall to simulate turbine airfoil film cooling is wrong, and the results are misleading. Again, the physics of a hot airfoil in a conjugate airfoil cooling condition is totally different from the hot airfoil with an internal heated source. In the conjugate case, the temperature of the hot wall is the consequence of the penetration of heat from the main stream gas and the spreading of this heat through the metal wall; this means that the hot airfoil temperature is passively achieved. This is very different from the hot surface produced by an actively heated source, which generates heat as an energy source no matter what the film cooling effect is. Evidence can be found from the negative  $\phi$  values generated upstream from the film hole of the heated wall case, which is not seen in the conjugate case or the cooled wall case. The heated wall acts as an active heat source and, as a result, the concept of using  $T_{aw}$  as the driving temperature potential is no longer valid since a competing heat source is added into the system and heat transfer on the airfoil is not solely determined by  $T_{aw}$ . Consequently, using  $T_{aw}$  in the heated wall film cooling analysis compounds the problems that could lead to negative  $h_{af}$  values when Eq. 3 is used.

The heated wall can be used as the correct boundary condition only if the heat flow direction is consistently reversed, i.e. using a heating jet with a temperature higher than the main gas stream ( $T_j > T_g$ ).

### Film Heat Transfer Coefficients

Although, the conventional practice of using a heated wall condition to simulate film cooling has been discussed earlier in

this paper as not physically correct, it is interesting to investigate how the  $h_{af}$  would be affected under these inappropriate conditions.

Heat Transfer Coefficient without Film --- The  $h$ -value without a cooling film is investigated for six 2D cases of different boundary conditions including a conjugate case, two constant temperature wall cases (325K and 375K), uniformly cooled and heated wall cases ( $+3\text{kW/m}^2$  and  $-3\text{kW/m}^2$ ), and a strongly cooled ( $+6\text{kW/m}^2$ ) wall case. Note that the negative sign is used for a heated wall based on the definition that the positive heat flux direction is assigned from the gas to the wall. The results are compared in Fig. 6 with the well established correlation for forced turbulent convection on a flat plate [15]:

$$Nu_x = 0.029 Re_x^{0.8} Pr^{0.4} \quad (10)$$

It is found that all the results are higher than the turbulent correlation of Eq. 10. Both constant wall temperature wall cases and the uniformly heated case achieve lower  $Nu$  than the conjugate case. A change of constant temperature wall cases from  $T_w = 325\text{K}$  to  $375\text{K}$  leads to a change of 5% in  $Nu$ . This corresponds to a 50% change in the wall temperature boundary condition based on the temperature scale  $T_g - T_j = 100\text{K}$ . Uniformly cooled cases result in 6-12% higher  $Nu$ . In summary, the change of the wall boundary condition affects  $Nu$  within an envelope of  $\pm 12\%$  centered at the conjugate case with a no-film condition.

Heat Transfer Coefficient with Film-Cooling --- It needs to be noted that the definition of  $h_{af}$  is built upon the concept of adiabatic wall temperature as  $h_{af} = q'' / (T_{aw} - T_w)$ . The adiabatic wall temperature must be known before  $h_{af}$  can be acquired.

The film-cooling heat transfer coefficient and corresponding Nusselt numbers for different boundary conditions are shown in Fig. 7 (a) and (b), and the ratio of ( $h_{af}/h_o$ ) for all cases are shown in Fig. 7 (c). Comparing with the no-film cases, the value of  $h_{af}$  has increased about 100% from  $h_o$  for most of the cooling surface. Near the injection hole region, the  $h$ -value is enhanced as much as 500%. Nusselt numbers for the two uniformly cooled cases are almost identical to the conjugate case. For the heated wall case,  $Nu$  is lower than the conjugate case and the difference can be as high as 15%.

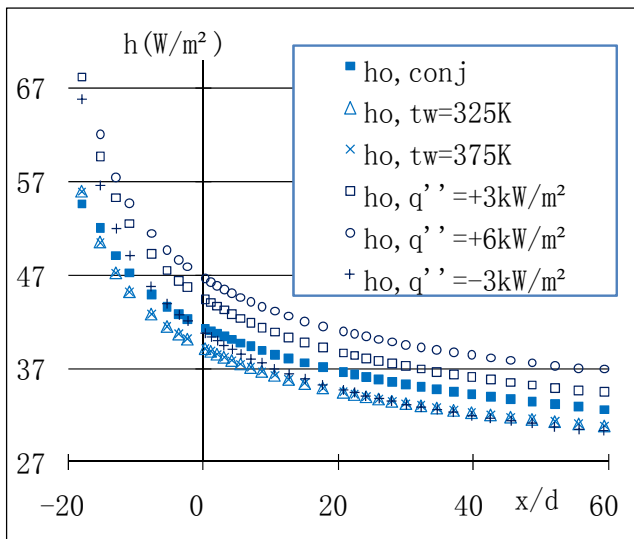
Divergence of  $h_{af}$  is found for conjugate case at  $x/d \approx 5.6$  and constant temperature wall ( $T_w=325\text{K}$ ) case at  $x/d=38$ . The divergence of  $h_{af}$  arises from the mathematical treatment of  $h_{af}$  at zero heat flux. As  $h_{af}$  is defined as  $h_{af} = q'' / (T_{aw} - T_w)$ , when  $T_w$  approaches  $T_{aw}$ ,  $h_{af}$  diverges. Figure 5a shows the wall temperature profiles of both the conjugate case and the constant wall temperature case ( $T_w=375\text{K}$ ) intercept the curve of the adiabatic wall temperature. The locations of the interceptions are where the divergence of the  $h_{af}$  value occurs. This implies that using  $h_{af}$  will encounter mathematical problem in the actual conjugate airfoil cooling condition if the local  $T_w$  approaches  $T_{aw}$ . Having been explained before, this is caused by the reverse heat conduction in the wall.

In the introduction section, the concern of using the isoenergetic jet film heat transfer coefficient as the adiabatic film cooling coefficient ( $h_{af}$ ) was expressed because the effect of the coolant jet temperature is not included in the heat transfer coefficient. To investigate this issue, an additional case using an isoenergetic jet was computed by CFD and shown in Fig. 7 (a). As can be seen, the  $h_{af}$  value of the isoenergetic jet case is about

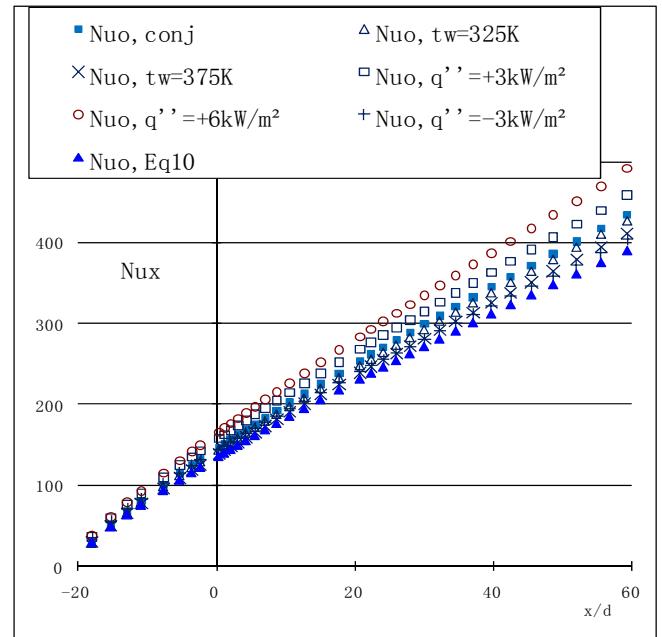
20-25% lower than the cooling jet conjugate case. Considering that  $T_w$  of the isoenergetic case should be higher due to the lack of a low-temperature jet protecting the surface, it seems strange that the isoenergetic case has lower  $h_{af}$  values. A further investigation reveals another problem of using the isoenergetic case to determine  $h_{af}$ : What  $T_{aw}$  value should be used in Eq.3 to calculate the  $h_{af}$  value for the isoenergetic case? Based on the actual physics, the true  $T_{aw}$  should be  $T_g$  in the isoenergetic case, so the  $h_{af}$  values for the isoenergetic case in Fig. 7(a) are obtained from using  $T_{aw} = T_g$ . However, since Eq. (1) was derived using only one  $T_{aw}$  value, this dictates the necessity of using the same  $T_{aw}$  as obtained from the adiabatic wall case (Case2) in Eq.3 for calculating the  $h_{af}$  value of the isoenergetic case. However, if this  $T_{aw}$  from Case2 is used, some of the  $h_{af}$  values become negative in the 2D cases (not shown) because some wall temperature values are higher than the  $T_{aw}$  values while the heat flux is positive (from gas to wall). The appearance of these negative  $h_{af}$  values further brings into question the adequateness of the practice of using the isoenergetic case to obtain the  $h_{af}$  values.

Film injection exerts a strong effect on  $h_{af}$  augmentation near the injection hole region. But, different thermal boundary conditions investigated in this study do not seem to impose noticeably different effects on  $h_{af}$  in the near-hole region. This is not unexpected because the film cooling effect is supposed to be strong and dominated by the flow behavior, not the thermal boundary condition immediately downstream of the injection hole. If the blowing ratio or the blowing hole geometry changes, the film effectiveness would have a more discernable difference because the flow structure would be altered. As the flow moves further downstream, the effect of the thermal boundary condition becomes more discernable.

Similar explanation can be made for the relatively lower  $h_{af}$  from the heated wall condition case, comparing with the cooled wall cases. The cooling wall will take the heat out of the film, which is continuously heated by the main stream, and thus helps to distinguish the coolant film from the main hot gas. Fig. 7c shows the trend of the ratio of  $h_{af}/h_o$  is similar to  $h_{af}$  (Fig. 7a), but with less variation from case to case.

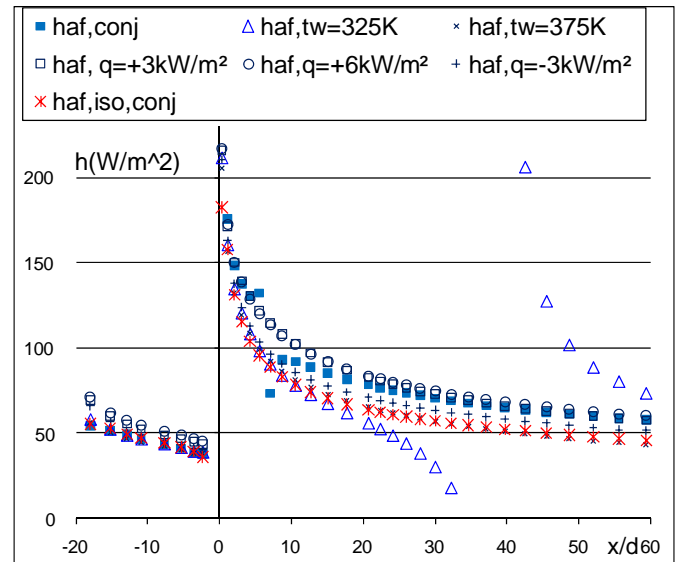


(a)



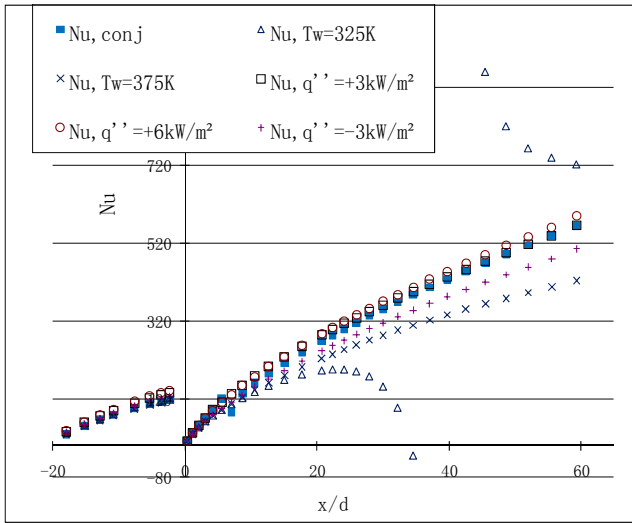
(b)

Figure 6 Heat transfer coefficient of without-film cases (a) Nu (b) h-value

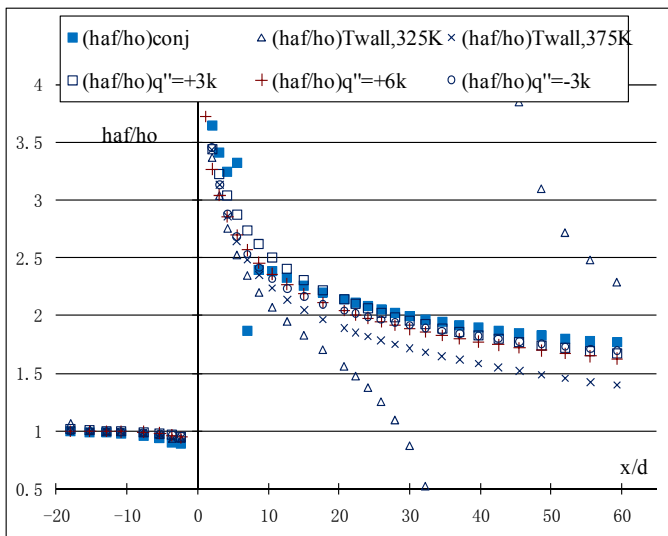


(a)  $h_{af}$  comparison





(b) Nu comparison



(c)  $h_{af}/h_o$  comparison

Figure 7 Comparisons of cases of different boundary conditions: (a)  $h_{af}$ , (b) Nu, (c)  $h_{af}/h_o$

In summary, the conventional practice of using a uniformly heated wall as the boundary condition to simulate film cooling conditions, although it does not provide correct physics, can provide the  $h_{af}$  value within 10-15% of the conjugate case value. The isoenergetic jet heat transfer coefficient is about 20-25% off from the cooling jet conjugate case. The uniformly cooled wall cases fair better than heated cases. Near the film hole ( $x/d < 6$ ), the variation of the  $h_{af}$  values from different thermal boundary conditions diminishes. Calculation of  $h_{af}$  will encounter an undefined condition when  $T_w$  approaches  $T_{aw}$ . But, ironically, this does not happen to the heated wall cases because  $T_{aw}$  is always higher than  $T_w$ . It needs to be remembered that even though the  $h_{af}$  and  $h_{af}/h_o$  results of heated and cooled cases are within 20% of the conjugate value, the  $\phi$  value can be 100-200% off (see Fig. 5b).

### 3D Studies

So far, the discussions have been based upon results from 2D studies. To further investigate those raised issues, 3D

simulations are carried out. Wall temperatures of different boundary conditions are plotted in Fig. 8 (a) and their corresponding non-dimensional form in Fig. 8 (b).

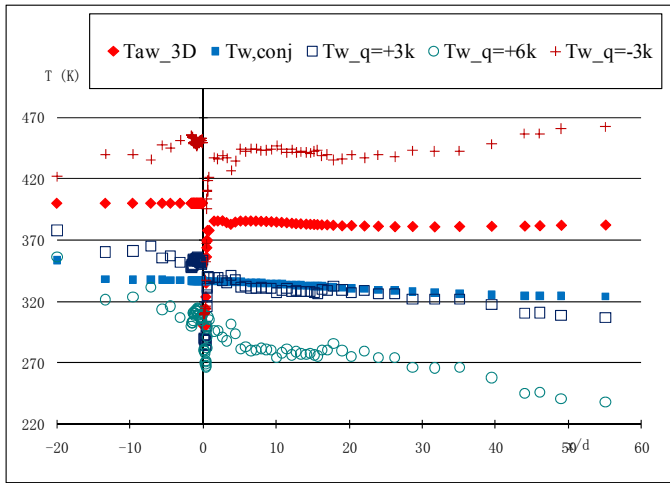
It is noticed that under the heated wall condition, the wall temperature is higher than the adiabatic wall temperature; as a result, unrealistic negative  $\phi$  values prevail over the entire surface as shown in Fig. 8 (b). Again, this is caused by the unrealistic heat source that has been added to the system which does not exist in an operating gas turbine system. The  $\phi$ -values in the 3D conjugate case and  $\eta$ -values in the 3d adiabatic wall case in Fig. 8(b) are significantly lower than the corresponding values of 2D cases in Fig. 5(b). The  $\eta$ -value drops very quickly from unity at the cooling injection hole to about 0.25 within 2-hole diameter distance downstream in the 3D case; whereas the decreasing rate of  $\eta$  in the 2D case is much slower, changing from unity to about 0.85 further downstream. In the 3D conjugate case,  $\phi$  actually increases from a value about 0.6 near the cooling hole to 0.75 further downstream at  $x/d=55$ . This is opposite to the decreasing trend of  $\phi$  in the 2D case.

Similar to the 2D case, the 3D uniformly cooled case with  $q''=6kW/m^2$  results in unrealistic  $\phi$ -values larger than unity; however, the 3D uniformly cooled case with  $q''=3kW/m^2$  fairs relatively well with the 3D conjugate case (Fig. 8b), which is not seen in the 2D case (Fig. 5b).

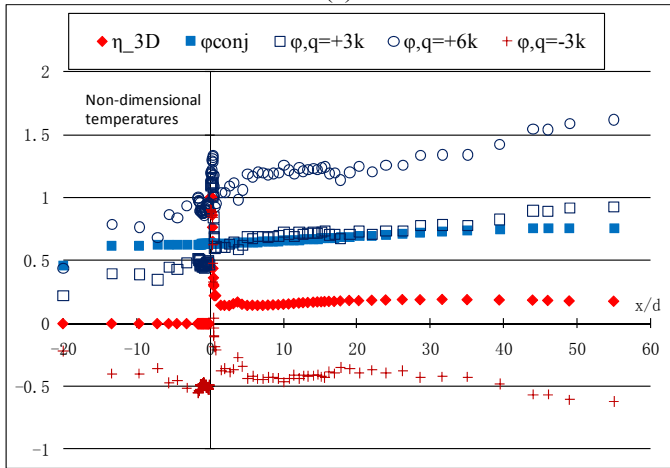
The afore-mentioned differences between 3D and 2D cases are attributed to the complex 3D film cooling flow structure including the strong vortices induced lateral flow mixing. Since the objective of this study is not focused on investigating the 3-D film cooling flow structure, more detailed discussion of the secondary flow structure in film cooling flow is referred to Haven and Kurosaka [16].

In Fig. 8, the zero heat flux point is expected to be at the location where  $T_{aw}$  intersects with  $T_w$  in the conjugate case. Noticing that the  $\phi$  value for the conjugate case is about the same as the cooled wall case ( $q''=+3kW/m^2$ ), it suggests that the cooling power on the airfoil is about the same for both cases in 3D flow.

The adiabatic film heat transfer coefficients of the 3D cases are plotted in Fig. 9. Again, the divergence of  $h_{af}$  under the conjugate condition is found very close to the injection hole, which is the location where  $T_w$  approaches  $T_{aw}$ . Among the constant heat flux wall conditions, the strongly cooled wall case gives the highest  $h_{af}$  and the difference is less than 14% of the conjugate  $h_{af}$ . In the area of  $x/d < 20$ , a discrepancy in the  $h_{af}$  values is found between the conjugate wall with internal cooling and constant heat flux wall conditions. The difference can be up to 50% of the  $h_{af}$  value from the conjugate case. The conjugate wall's conduction effect, which does not exist in the simulation of the heated or cooled wall case, smears the temperature difference within the blade, thus affecting the nearby air flow and reducing the heat transfer coefficient. The airfoil surface temperature contours of the conjugate case, isoenergetic case, and heated wall case are shown in Fig. 10. In the region further downstream of the film injection hole,  $h_{af}$  of the isoenergetic case is higher than that of the conjugate case. The  $h_{af}$  values of the isoenergetic cases are obtained using the same  $T_{aw}$  that is used in the adiabatic wall case. If the  $T_g$  value is used as  $T_{aw}$ , because the true adiabatic wall temperature is  $T_g$  in the isoenergetic case, the  $h_{af}$  values will be about 20-40% lower.



(a)



(b)

Figure 8 3D (a) adiabatic wall temperature and wall temperature (b) film cooling effectiveness ( $\phi$ ) and adiabatic film cooling effectiveness ( $\eta$ ) under different wall conditions.

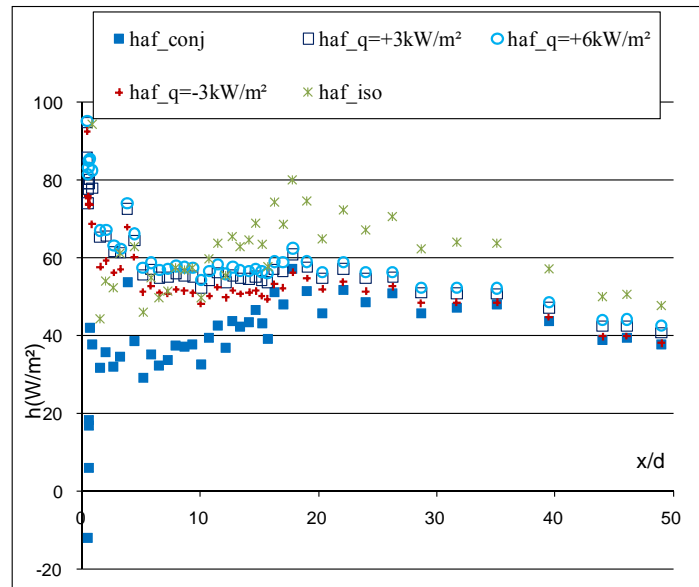
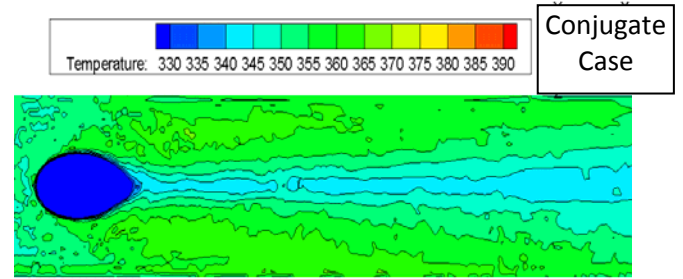
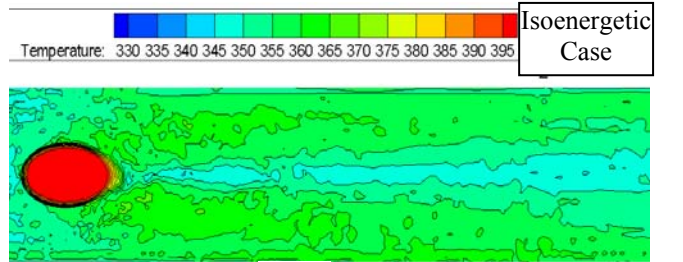


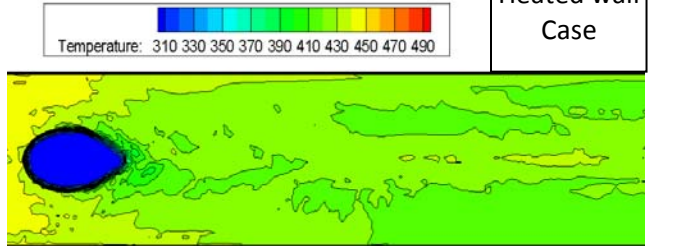
Figure 9 Adiabatic Film Heat transfer coefficients ( $h_{af}$ ) of 3D Cases



(a)



(b)



(c)

Figure 10 Airfoil surface temperature contour of the (a) conjugate case (b) isoenergetic case (c) heated wall case with  $q'' = -3\text{kW/m}^2$

## CONCLUSION

In this study, the practice of employing a heated surface to simulate the actual film-cooling condition is closely investigated. Considering that the dominant energy passage in turbine airfoil film cooling is always from the hot combustion gas flowing into the airfoil, employing a heated surface to simulate the actual film cooling condition does not seem to provide the correct physics. A series of computationally simulated cases have been designed in this study to systematically investigate the consequent issues of employing a heated surface.

It is shown that under the heated wall condition, a negative film-cooling effectiveness can be found as a result of a higher surface temperature than the main gas stream temperature, which is unrealistic for an operational turbine system. The concept of using the adiabatic wall temperature ( $T_{aw}$ ) as the driving temperature potential is no longer valid because an artificially created competing heat source (the heated wall) is added into the system, and the heat transfer mechanism on the airfoil is not solely determined by  $T_{aw}$ .

Heating the surface to simulate the film cooling boundary condition, although it does not provide the correct physics, can provide the heat transfer coefficient value within 10-15% of the value calculated from the correct boundary conditions. Using a heated surface is only correct under one condition: when all the conditions are reversed, i.e. with a hot jet and cold main gas flow.

It is also found that the calculation of  $h_{af}$  will be undefined when  $T_w$  approaches  $T_{aw}$  under the heated wall condition. The isoenergetic jet heat transfer coefficient is about 20-25% off

from the cooling jet conjugate case. The uniformly cooled wall cases fair better than heated cases.

#### ACKNOWLEDGEMENT

This study is supported by the Louisiana Governor's Energy Initiative via the Clean Power and Energy Research Consortium (CPERC) and administered by the Louisiana Board of Regents.

#### REFERENCE

- [1] W.J. Mick, R.E. Mayle, Stagnation film cooling and heat transfer, including its effect within the hole pattern, *ASME J. of Turbomachinery* 110 (1988) 66-72.
- [2] The Gas Turbine Handbook, Office of Fossil Energy, National Energy Technology Laboratory, U.S. Department of Energy, 2006, PP. 310-318.
- [3] S. W. Burd, C. J. Satterness, and T.W. Simon, Effects of bleed injection over a contoured end wall on nozzle guide vane cooling performance: part II – thermal measurements, *ASME TurboExpo 2000*, 2000-GT-200
- [4] D.R. Thurman, P.E. Poinsette, and J.D. Heidmann, Heat transfer measurements for a film cooled turbine vane cascade, *ASME TurboExpo 2008*, GT2008-50651.
- [5] M. Jonsson, D. Charbonnier, P. Ott and J. von Wolfersdorf, Application of the transient heat foil technique for heat transfer and film cooling effectiveness measurements on a turbine vane endwall, *ASME TurboExpo 2008*, GT2008-50451.
- [6] M. Nicklas, Film-Cooled Turbine Endwall in a Transonic Flow Field: Part II- Heat Transfer and Film Effectiveness, *ASME J. of Turbomachinery*, 123, pp. 720-729, 2001.
- [7] B.D. Mouzon, E.J. Terrell, J.E. Albert, D.G. Bogard, Net heat flux reduction and overall effectiveness for a turbine blade leading edge, *ASME TurboExpo 2005*, GT2005-69002.
- [8] S.M. Coulthard, R.J. Volino, K.A. Flack, Effect of Jet Pulsing on Film Cooling-Part II: Heat Transfer Results, *ASME J. Turbomachinery* 129 (2007) 232-246.
- [9] K.M. Womack, R.J. Volino and M.P. Schultz, Measurements in film cooling flows with periodic wakes, *ASME TurboExpo 2007*, GT2007-27917.
- [10] T. Wang and L. Zhao, A Revised Equation for Calculating Heat Flux Reduction in Film Cooling Studies, GT2011-45953, manuscript submitted to *ASME Turbo Expo 2011*, Vancouver, Canada, June 6-10, 2011
- [11] C.M. Bell, H. Hamakawa, P.M. Ligrani, Film cooling from shaped holes, *ASME J. Heat Transfer*, 122 (2000) 224-232.
- [12] R.A. Brittingham, J.H. Leylek, A detailed analysis of film cooling physics: Part IV—compound-angle injection with shaped holes, *ASME J. Turbomachinery* 122 (2002) 133-145.
- [13] *Fluent Manual*, Version 6.2.16, Fluent, Inc. 2005.
- [14] R. J. Goldstein, P. Jin, and R. L. Olson, Film Cooling Effectiveness and Mass/Heat Transfer Coefficient Downstream of One Row of Discrete Holes, *J. Turbo mach.* 121 (1999), 225-232
- [15] P.H. Oothsuzen, D. Naylor, *An Introduction to Convective Heat Transfer Analysis*, second ed, McGraw-Hill, New York, 1999
- [16] B.A. Haven, M. Kurosaka, Kidney and anti-kidney vortices in crossflow jets, *Journal of Fluid Mechanics*, 352 (1997) 27-64.